Numerical modeling and management of saltwater seepage from coastal brackish canals in southeast Florida

M. Koch[a], G. Zhang[b]

[b]*Department of Geohydraulics and Engineering Hydrology, University of Kassel, Kurt-Wolters Straße 3, D-34109 Kassel*

[b]*Geophysical Fluid Dynamics Institute, Florida State University, Tallahassee, FL, 33206*

Abstract

The phenomenon of density-driven vertical salt water intrusion from brackish open sea-canals in southeast Florida has been simulated with a density-coupled groundwater flow and transport model. The underlying conceptual model includes seasonal changes of the groundwater level, tidal variations of the canal stage, rainfall recharge, and a low permeability canal bed. As expected, whether brackish canal water intrudes into the aquifer, depends on the adjacent groundwater table elevation: lowering the latter during a dry season may initiate the seepage process which then becomes essentially irreversible. A significant influence of the short-term tidal fluctuations on the long-term dispersion of the vertical saltwater plume in the aquifer is found. The model is applied to simulate how the large Hollywood well field affects salt water intrusion from the adjacent C-10 tidal canal, and to determine possible mitigating water management strategies to prevent further intrusion. The models show that, for attaining this objective, a minimum threshold water level must be maintained in the well field during the dry seasons. However, raising the water table cannot be achieved by artificial injection of reclaimed wastewater, but may be accomplished by placing a freshwater canal along the brackish C-10 tidal canal.

1. Introduction

Salt water intrusion has been of concern in southeast Florida for some time *(Henry, 1964; Segol and Pinder, 1976; Andersen et al., 1989; Zhang, 1995)*. In addition to classical, horizontal oceanic intrusion which in Florida, as well as in many other coastal aquifers, has become an alarming problem due to increasing groundwater pumping (saltwater upconing), the situation in southeast Florida is exacerbated by the presence of numerous open canals connected to the Atlantic Ocean (*Fig. 1*). These canals serve as waterways for boat owners and/or flood control drainage. They often carry brackish, saline water from the ocean, especially during high tides. The salinity in the canal increases during the annual dry season when, as a consequence of a lowered groundwater table, the natural groundwater inflow into the canal is reduced and the hydrostatic balance between the saline canal and the fresh ambient groundwater is disturbed. Saltwater intrusion from the canal into the surficial aquifer may occur under such unfavorable conditions (*Chin, 1990)*.

This adverse situation is accentuated for brackish canals close to the wellfields in the region, such as the C-10 canal in the vicinity of the Hollywood wellfield *(Fig. 1)*. Brackish water has been detected in some of the the wells there (*Bearden, 1974)* limiting their use for the groundwater supply. The prediction of the future migration of the saltwater intrusion plume and the development of mitigating management strategies are of utmost importance for securing the groundwater supply in the area. Numerical models are the most efficient tools for this task, allowing the simulation of various scenarios.

In this paper the density-coupled flow and transport model SUTRA *(Voss, 1988)* will be used. In the first part of the paper the general characteristics of the canal intrusion process are investigated by means of a sensitivity analysis. In the second part the model is applied to test several management strategies on how to inhibit or to revert future saltwater intrusion.

The phenomenon of infiltration of saltwater into an aquifer is one representative of the general class of density-driven instability problems in miscible transport, the study of which has been of growing interest in recent years for practical purposes as well as for their peculiar theoretical aspects. Density effects on the migration of contaminant plumes have been observed by *Paschke and Hoopes (1984)* and numerically modeled by *Koch and Zhang (1992)*. Experimental investigations of variable density flow and mixing in porous media have been carried out by *Schincariol and Schwartz (1990)*. A numerical analysis of the physics underlying this so-called Rayleigh-Taylor instability problem was presented by *Koch (1992)* where it was found that the hydrodynamic dispersion was a major controlling factor of the instability.

2. Mathematical and numerical formulation

Flow in a porous media is governed by *mass-conservation (continuity)*

$$\frac{\partial (n\rho)}{\partial t} + \nabla \cdot (n\rho \mathbf{v}) = Q \,, \qquad (1)$$

and *Darcy's law* for the flow (seepage)-velocity v [L/T]

$$\boldsymbol{v} = -\frac{k}{n\mu}(\nabla p + \rho g \boldsymbol{k}_z) \qquad (2)$$

which results in the *groundwater flow equation* for the pressure p [M/LT^2]

$$S_0 \rho \frac{\partial p}{\partial t} + \left(n \frac{\partial \rho}{\partial c} \right) \frac{\partial c}{\partial t} = \nabla \cdot \left(\frac{k\rho}{\mu} (\nabla p + \rho g \boldsymbol{k}_z) \right) + Q \qquad (3)$$

(cf. Bear, 1979; Voss, 1984). Notations are: n porosity; ρ [M/L^3] density; μ [M/L/T] dynamic viscosity; k [L^2] permeability; g [L/T^2] gravity acceleration; Q [M/L^3/T] flow source/sink term; $\mathbf{k}_z$ vertical unit vector; $S = (1-n)\,\alpha + n\beta$ [LT^2/M] specific storativity; with α, β [LT^2/M], the compressibility of the aquifer matrix and of water, respectively.

The concentration c is described by the solute transport equation

$$n\rho \frac{\partial c}{\partial t} + n\rho \boldsymbol{v} \cdot \nabla c = \nabla \cdot (n\rho D \nabla c) + Q_s \qquad (4)$$

where Q_s [M/L^3/T], a solute source/sink term; $\mathbf{D} = D^* + \alpha_T |\mathbf{v}| \delta_{ij} + (\alpha_L - \alpha_T) v_i v_j / |\mathbf{v}|$ [L^2/T] hydrodynamic dispersion tensor; D^* [L^2/T] molecular diffusion; α_L, α_T [L], longitudinal and transversal dispersivity, respectively.

The flow eq. (3) and the transport eq. (4) are coupled through an equation of state, $\rho = \rho(c)$ which can be linearized as $\rho = \rho_r + \partial\rho/\partial c^*(c - c_r)$, with ρ_r the reference density for pure water ($c_r = 0$), and $\partial\rho/\partial c$ a constant.

The coupled flow and transport eqs. (3) and (4) are solved by the well-known SUTRA (Saturated-Unsaturated-TRAnsport) (*Voss, 1984*) 2D finite element model. SUTRA can either be used in the horizontal x-y domain or in a vertical x-z cross-section of a saturated-unsaturated zone. The latter set-up is employed in the present application. The discretization of the x-z domain is done by means of 4-node quadrilateral elements. A bilinear approximation for p and c is used in each element and the classical Galerkin formulation of eqs. (3) and (4) is established. For each timestep the resulting linear matrix systems for the nodal unknowns p or c are solved consecutively by an efficient iterative conjugate gradient technique, after the corresponding updates for the density $\rho(c)$ and the seepage velocity $\mathbf{v}$ (eq. 2) have been made. The integration in time is performed by means of a fully implicit backward Euler method which is unconditionally stable. Nevertheless, because of the strong coupling of ρ, p, and c, the timesteps Δt have to be taken sufficiently small to ensure convergence and stability, especially in those models where the semidiurnal tidal variations of the canal gage are considered.

3. Sensitivity study of the canal intrusion process

3.1 Objectives

To understand the physical dynamics of the canal saltwater intrusion and its sensitivity to various geohydraulic model parameters, numerous simulations were run, to answer the following questions: 1) for a given ambient surficial groundwater head h_a above the canal stage what is the critical canal concentration c_{cr} that starts intrusion? 2) for a given canal concentration c_0 what is the minimal ambient groundwater head $h_{a,cr}$ that prevents intrusion? 3) what are the separate and combined effects of seasonal and tidal variations?

3.2 Conceptual model; boundary and initial conditions; input parameters

The basis cross-sectional conceptual model consists of an aquifer section 2500ft wide and extending 220ft deep from the surface to the base of the Biscayne aquifer and which is incised in the middle by a tidal canal of depth H_w=10 ft and width of 80 ft. This model area is discretized by an 81x21 finite element grid which is horizontally refined underneath the canal (*Fig. 2*).

Boundary conditions are as follows: *bottom boundary:* no flow; *left* and *right boundaries:* periodically varying pressure that simulates seasonal changes of the ambient groundwater table (period T_s =12 months; i.e. $p_a = p_o$* *sin* $(2\pi t / T_s)$); *top boundary:* specified only at the position of the canal as periodically varying pressure due to the semidiurnal tidal gage height variations. In the brackish canal a Dirichlet b.c., $c = c_0$ for the chloride concentration is also prescribed when solving the transport eq. (4). An average annual rainfall recharge of 12 inches for the region is included by assigning the upper boundary appropriate source nodal values. As for the initial condition, the concentration is set to $c_i = 0$ throughout the aquifer, simulating the intrusion of brackish water into a fresh groundwater aquifer.

Further aquifer parameters are set as follows (*Zhang, 1995*): *Porosity* n =0,25; *aquifer compressibility* $\alpha = 10^{-9}$ ms^2/kg; *horizontal permeability* k_x = 1,9 x 10^{-11} m^2; *vertical permeability* k_z = 1,9 x 10^{-11} m^2 ; *longitudinal dispersivity* α_L = 1m; *transverse dispersivity* α_T = 0,1 m.

3.3 Simulation results

Fig. 3 illustrates results of the simulation family P2 answering question 1) above. The ambient head h_a is fixed to 1m above canal stage (see *Fig. 2*) and is time-invariant, i.e. neither seasonal nor tidal variations are included here. Saltwater fronts are shown after 15 years for two canal chloride concentrations of c_0=13000 and c_0=15000 ppm, respectively. Whereas for the former case, no intrusion is observed, for c_0 = 15000 ppm the plume has not only sunk to the bottom of the aquifer, but has also widely spread horizontally. Thus, for a head h_a=1m the critical concentration is c_{cr} ~14000 ppm. Of course, increasing h_a will result in yet higher values of c_{cr} for intrusion to occur.

By reverting the above reasoning, question 2) will be answered in the simulation family P4. Here c_0 is fixed at 13000 ppm and, in order to mimic seasonal changes, the ambient groundwater table h_a is varied periodically with an amplitude of 0.5m around an average head h_{a0} which is altered within this simulation set. Note that tidal effects are still discarded here. *Fig. 4* shows that

whereas for h_{ao} = 1.1ft the plume has fully penetrated into the aquifer after 15 years, canal intrusion is inhibited by merely increasing h_{ao} to h_{ao} = 1.2 ft. The latter thus represents the critical average groundwater table height h_{a0cr} that must be maintained permanently to prevent intrusion. It should be noted that for the same model without seasonal changes, h_{a0cr} is only about 0.8ft (*Zhang, 1995*). The higher value found for the average head h_{a0cr} in the former simulation set P4 is required to counterbalance the accelerated intrusion during the dry-season interval with lower-than-average water table heights.

The additional effects of semidiurnal tidal variations of the canal gage are illustrated in the model set P10. Because of the very small timesteps Δt <3h required for the resolution of the tides, the integration was only carried out up to 10 years. Following observed tides in the New River (*Fig.1*), a tidal amplitude of 1.5ft is used for the canal b.c., on top of the seasonal variations of model set P4. *Fig.5* depicts two cases with different average groundwater heights h_{ao}. Whereas no canal intrusion is obtained after 10 years for h_{ao} = 1.8ft, the saline plume has fully seeped into the aquifer for h_{ao} = 1.2ft, so that the former value is the critical height h_{a0cr} required to permanently prevent canal intrusion.. Note that this value of h_{a0cr} is higher than the h_{a0cr} =1.2ft obtained previously for model set P4 which included only seasonal groundwater changes. The short-periodic canal tides have therefore a non-negligible effect on the long-term canal intrusion. Visual differences are also observed in the plume contours of the two simulation sets P10 (*Fig. 4*) and P4 (*Fig.5*) which are smoother in the former (with tides) than in the latter case (no tides), providing evidence for a larger effective hydrodynamic dispersion generated by the high-frequency tidal velocity fluctuations.

4. Application to the C-10/Hollywood field area

4.1 Effects of the Hollywood groundwater pumping

The foregoing results demonstrate that canal intrusion will occur only if the groundwater level falls temporarily, e.g. during a dry season, below a critical threshold. Clearly, heavy groundwater pumping close to a canal will magnify such a situation. This appears to be the case for the C-10 canal/ Hollywood wellfield (HW) area (*Fig. 1*), where Chloride (Cl^-) concentrations of ca 10000 ppm in the canal and ca 500 ppm in the aquifer have been detected (*Bearden*, 1974). Geophysical resistivity surveys have delineated a foot-shaped saline plume between the C-10 and the HW (see *Zhang, 1995,* for details).

To investigate the effects of the HW on the future migration of this intrusion, several models similar to the ones before were run, but which mimic an 8400 ft wide aquifer cross-section starting west of the HW and extending east of the C-10 (see *Fig. 1*) and that include pumping of the HW. Because its wells extend essentially in the NS- direction, parallel to the C-10, the HW can be modelled as a line source, and the 2D model approach is applicable.

Fig. 6 shows the intrusion fronts after 20 years for a model with the present-day pumping rate Q_p of the HW (27.6mgd) and another one with twice that value ($Q_f = 2*Q_p$), representing anticipated future groundwater demands. Both seasonal and tidal variations are included and a canal Cl^--concentration of 6000ppm is assumed. The model is calibrated for the aquifer permeability and the dispersivity, using head- and Cl^--measurements in the two monitor

wells G-1240 and G-1548 located between the HW and the C-10 canal.

The notable feature of *Fig. 6* is the insensitivity of the $0.1c/c_0$ isoline (≙600ppm which are above the 250ppm Florida Drinking Water Standard) to the pumping rates Q_p and Q_f. Contrary to expectation, the toe of that isoline for the double Q_f pumping has not intruded further than that for the present-day Q_p. The time histories of the intrusion fronts show (*Zhang, 1995*) that for both models these have reached approximately steady-state after 20 years.

4.2 Management of canal intrusion using hydraulic barriers

Although the previous results indicate that increasing the pumping rate in the HW should not trigger a further advance of the present-day C-10 brackish intrusion front, the question arises if and what kind of management strategies can be taken to stop or even revert intrusion. The models discussed so far suggest that to attain this objective, a sufficiently high groundwater table has to be created, especially during dry seasons. Two variants of such a "hydraulic barrier", whose effectiveness and practicality will be tested in this section are: (1) aquifer injection of reclaimed wastewater, proposed by Floridan agencies, which would create a permanent groundwater mound; (2) construction of a freshwater canal whose gage height h_c would be maintained at an all-season sufficiently high level, with the effect of also raising the groundwater table.

For the numerical test of the injection barrier model (1), an injection well with a recharge rate equal to the today pumping of the HW (27.6mgd) was placed as a source node 120m deep in the aquifer, halfway between the HW and the C-10 canal. Since all other model parameters are identical to those used in the previous section, the effects of such an injection well on the intrusion fronts can be directly seen by comparing *Fig.7, Top* with *Fig. 6, Top.* Obviously, even after 20 years of simulation the $0.1\ c/c_0$-isoline for the injection model in *Fig.7, Top* has barely retreated from its former position in *Fig. 6, Top.* Other models with higher injection rates were run, but could not improve this negative outcome much neither. Therefore, one can conclude that this injection variant of the hydraulic saltwater barrier is not a viable option, given also the huge quantities of reclaimed wastewater that would be needed.

The freshwater canal option (2) is modeled by imposing a Dirichlet bc. $h = h_c$, for a top boundary node at the hypothetical canal position , midway between the HW and the C-10 (width of 100 m). The average canal stage height h_c was chosen as $h_c = 1.6$ ft which is sandwiched between the seasonal changes of the groundwater table, ensuring the natural canal recharge from the aquifer during the wet season, but raising the groundwater table during the critical dry season. The effectiveness of such a 'hypothetical' freshwater canal can be clearly seen from *Fig. 7, Bottom.* Compared with the reference model of *Fig. 6, Top,* after 20 years, the saltwater intrusion plume has been pushed back towards the brackish canal and has maximum concentrations $c/c_0<0.1$. A budget analysis shows that the amount of freshwater infiltrating from the hypothetical canal into the aquifer during the dry season is about 9 times the today HW pumping rate. Although a portion of this fresh canal water is naturally flowing back out of the aquifer during the wet seasons, additional surficial water will be needed to make this kind of hydraulic barrier feasible.

References

Andersen, P.F.,J.W. Mercer and H.O. White, Numerical modeling of saltwater intrusion in Hallandale, Florida, *Groundwater*, 26, 203-210, 1989.

Bear, J., *Hydraulics of groundwater*, Mc Graw Hill, New York, 1979.

Bearden, H.W., Groundwater resources of the Hollywood area, Florida, *USGS Water Resources Investigations Report*, 74-015, 1974.

Chin, D.A., A method to estimate canal leakage to the Biscayne aquifer, Dade county, Florida, *USGS Water Resour. Invest. Rep.*, 90-4135, 1990.

Henry, H.R., Effects of dispersion on salt encroachment in coastal aquifers, *US. Geol. Survey Water Supply Paper*, 1613-C, 1964.

Koch, M., Numerical simulation of finger instabilities in density and viscosity dependent miscible solute transport, In: *Proc. IX Int. Conf. Comput. Meth. Water Resour.*, Russel, T.F. et al. (ed.), pp. 155–162, Computational Mechanics Publications, Southampton, UK, 1992.

Koch, M., and G. Zhang, Numerical simulation of the effects of variable density in a contaminant plume, *Groundwater*, 5, 731-742, 1992.

Paschke, N.W., and J. Hoopes, Buoyant contaminant plumes in groundwater, *Water Resour. Res.*, 20, 1183–1192, 1984.

Schincariol, R.A., and F.W. Schwartz, An experimental investigation of variable density flow and mixing in homogeneous and heterogeneous media, *Water Resour. Res.*, 26, 2317–2329, 1990.

Segol, G. and G.F. Pinder, Transient simulation of saltwater intrusion in southeast Florida, *Water Resour. Res.*, 12, 65–70, 1976.

Voss, C.I., SUTRA, A finite element simulation model for saturated unsaturated fluid-density-dependent ground energy transport or chemically reactive single species solute transport, *U.S. Geol. Survey Water Resour. Investig. Report* 84–4369, 1984.

Zhang, G., Numerical models of saltwater intrusion from brackish canals in southeast Florida, *Ph.D. Thesis*, FSU, Tallahassee, Florida, 1995.

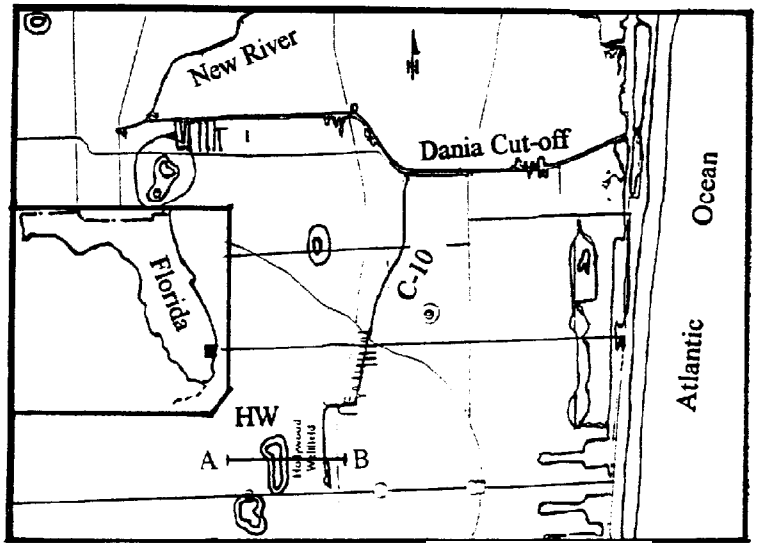

Fig. 1: Map of Broward county, with main tidal canals and the HW. The line AB marks the aquifer cross-section modelled in Section 4.

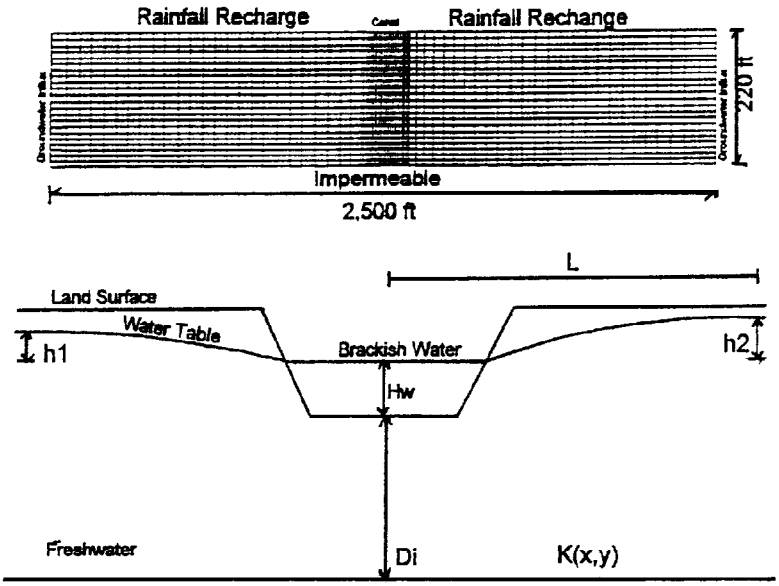

Fig. 2: Conceptual model of the canal intrusion process (Top panel) and the finite element grid used (Bottom panel) (not to scale)

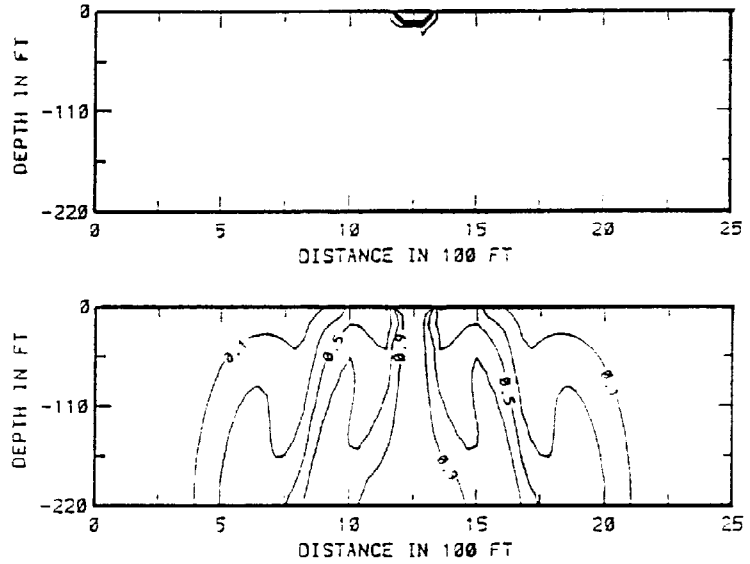

Fig. 3: Simulation set P2 with constant ambient groundwater head h_a = 1 m. Normalized (c/c_0) saltwater intrusion isolines after 15 years for Cl- concentration of c_0 =13000 (Top) and c_0 =15000 ppm (Bottom).

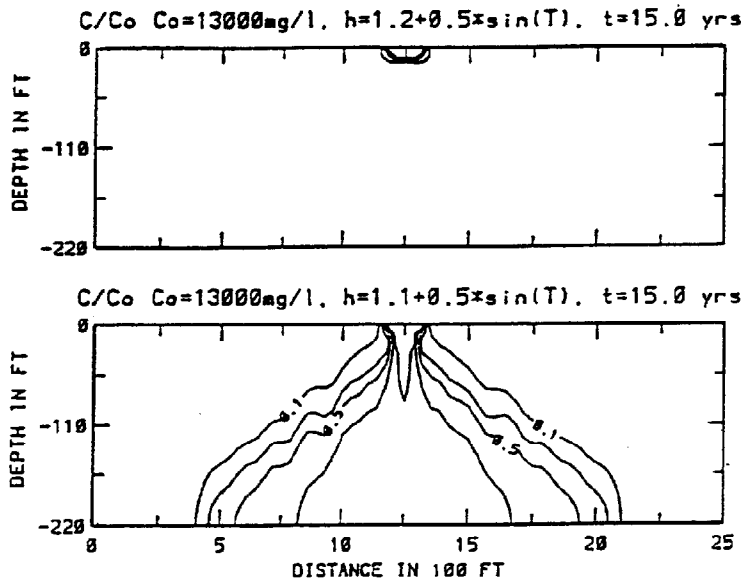

Fig. 4: Simulation set P4 including seasonal variations.Saltwater intrusion fronts after 15 years for two models with ambient groundwater head h_{a0} of 1.2m (Top) and 1.1m (Bottom), respectively.

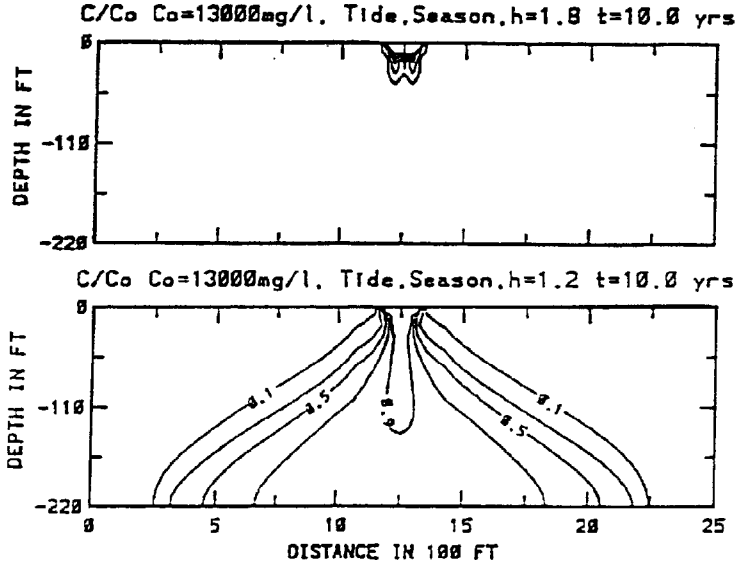

Fig. 5: Simulation set P10 including seasonal and tidal variations. Intrusion fronts after 10 years for two models with ambient groundwater heads h_{a0} of 1.8m (Top) and 1.2m (Bottom), respectively.

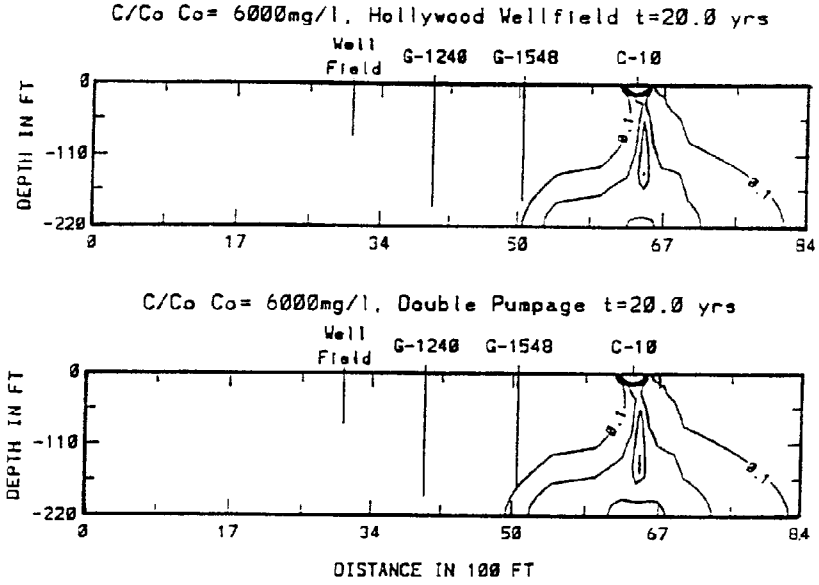

Fig. 6: Effect of pumping of the HW on the C-10 intrusion. Top: present-day pumping rate; Bottom: twice the present-day pumping rate

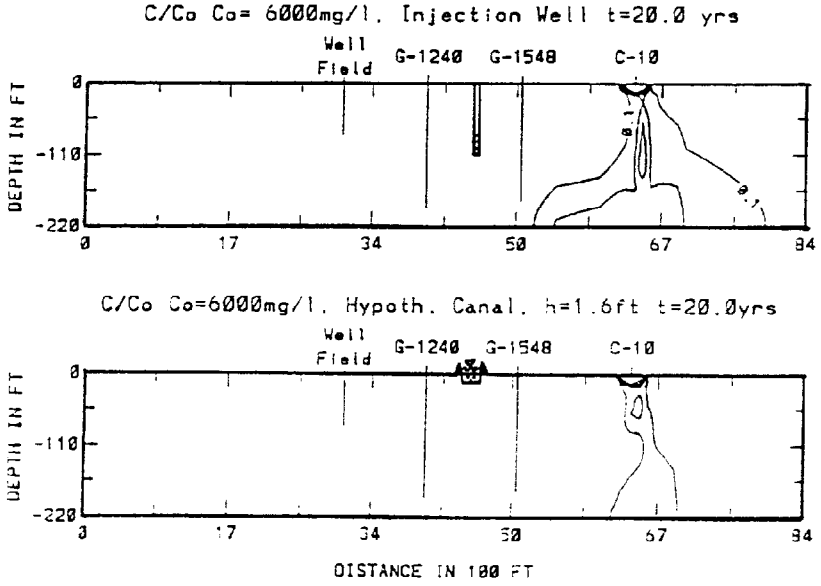

Fig. 7: Management of canal intrusion using hydraulic barriers. Top: Effect of an injection well; Bottom: Effect of a freshwater canal.